Title

COLLISIONAL ENERGY TRANSFER IN THE LOW PRESSURE LIMIT UNIMOLECUIAR DISSOCIATION OF HO2

Authors

Brown, N.J.
Miller, J.A.

Publication Date

1983-10-01

Lawrence Berkeley Laboratory
UNIVERSITY OF CALIFORNIA

APPLIED SCIENCE DIVISION

Presented at the Western States Meeting of the Combustion Institute, University of California, Los Angeles, CA, October 17-18, 1983

COLLISIONAL ENERGY TRANSFER IN THE LOW PRESSURE LIMIT UNIMOLECULAR DISSOCIATION OF HO_2

N.J. Brown and J.A. Miller

October 1983

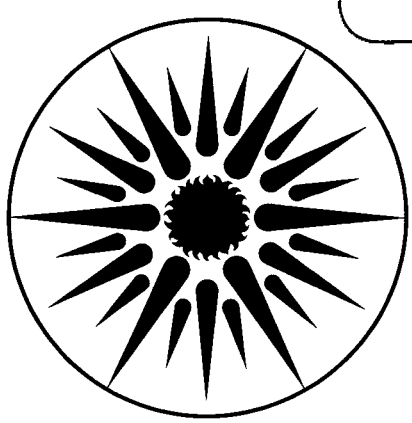

APPLIED SCIENCE DIVISION

Prepared for the U.S. Department of Energy under Contract DE-AC03-76SF00098

DISCLAIMER

LBL-16790

COLLISIONAL ENERGY TRANSFER IN THE LOW PRESSURE LIMIT UNIMOLECULAR DISSOCIATION OF HO_2

Nancy J. Brown
Applied Science Division
Lawrence Berkeley Laboratory
University of California
Berkeley, CA 94720

and

James A. Miller
Combustion Chemistry Division
Sandia National Laboratories
Livermore, CA 94550

This work was supported by the U.S. Department of Energy under Contract No. DE-AC03-76SF00098.

COLLISIONAL ENERGY TRANSFER IN THE LOW PRESSURE LIMIT UNIMOLECULAR DISSOCIATION OF HO_2

Nancy J. Brown
Applied Science Division
Lawrence Berkeley Laboratory
Berkeley, CA 94720

and

James A. Miller
Combustion Chemistry Division
Sandia National Laboratories
Livermore, CA 94550

ABSTRACT

Classical trajectory calculations are used to investigate the energy transfer properties of HO_2-He collisions under conditions where HO_2 is initially excited to energies near dissociation. The emphasis in this investigation is on determining the dependence of vibrational energy transfer characteristics on heat bath temperature, total molecular energy, and total molecular angular momentum. Vibrational energy transfer is a function of all three variables. Energy transfer averages, correlation coefficients, and energy transfer cross sections are used to determine the energy transfer mechanism. Evidence is found for all types of energy transfer, but the specific mechanism for a particular ensemble is highly dependent on the initial variables.

At fixed vibrational energy and heat bath temperature, the magnitude of the average vibrational energy transferred per collision, $|<\Delta E'>|$, increases with increasing molecular angular momentum. At fixed initial molecular angular momentum and heat bath temperature $-<\Delta E'>$ increases as the total energy in the molecule increases, except for very low values of initial angular momentum. Increasing the heat bath temperature for fixed values of the other initial variables decreases the magnitude of $<\Delta E'>$. The relative importance of weak and strong collisions in governing the energy transfer characteristics is discussed. In particular, the probability density function for vibrational energy transfer is not well represented by a simple "exponential down" model. A double exponential function is required to represent the long tail of the distribution adequately. Total vibrational energy transfer cross-sections determined from vibrational energy transfer histograms are weak functions of total energy, total angular momentum, and heat bath temperature. They are systematically higher than the corresponding Lennard-Jones cross sections.

COLLISIONAL ENERGY TRANSFER IN THE LOW PRESSURE LIMIT UNIMOLECULAR DISSOCIATION OF HO_2

I. INTRODUCTION

Thermal unimolecular dissociation, and the reverse recombination, reactions in the gas phase represent an important class of elementary processes in complex systems, particularly combustion. Recombination reactions typically are the most important source of heat in flames, and the dissociation of weakly bonded free radicals provides important mole number (i.e. number of molecules per unit mass) increases in combustion systems. Such mole number increases typically accelerate the oxidation process either by satisfying a thermodynamic requirement or by feeding chain branching reactions, or both. Obviously, it is desirable to understand this class of reactions.

In the high pressure limit of thermal unimolecular dissociation, intramolecular energy transfer processes are rate determining. However, in the low pressure limit collisional energy transfer to and from the dissociating molecule determines the rate coefficient. In the "strong collision" version of unimolecular rate theory, it is implicitly assumed that molecules below the dissociation limit are always in thermal equilibrium with the ambient heat bath. In this version of the theory the Arrhenius pre-exponential factor in the low pressure limit is determined primarily by the density of states at the dissociation limit, and the activation energy is normally very close to the bond energy (or threshold energy), or at least easily

related to it. However, discrepancies between strong collision theory and experiment have been known for a long time. It is not unusual for the dissociation rate coefficient of a molecule at high temperature to be as much as two orders of magnitude below that predicted by strong collision theory and for the activation energy to be several kcal/mole below the strong collision theory prediction. Such discrepancies are now known to be due to "weak collision effects". "Weak collisions" result in the transfer of relatively small quantitites of energy per collision with the result that bound energy states near the dissociation limit are unable to maintain equilibrium populations. These states are underpopulated during dissociation and overpopulated during recombination. This phenomenon results in the discrepancies between experiment and strong collision theory noted above.

Our current awareness of weak collision effects in polyatomic molecules is due largely to Troe[1−6], who has developed a formalism that can be used effectively to reduce, interpret, and extrapolate experimental data. He has also correctly pointed out[3] "that a substantial uncertainty persists because of the lack of knowledge of a number of input data such as details of potential energy surfaces or of intermolecular energy transfer processes." This lack of knowledge of collisional energy transfer processes in highly vibrationally excited polyatomic molecules is the primary motivation for this paper. There are two related investigations that deserve mention. Gallucci and Schatz[7] have studied the dynamics of He-HO_2 collisions for HO_2 molecules excited well above the dissociation limit. Since the dissociation limit in low presure limit unimolecular reactions represents a completely absorbing barrier, this regime is not of interest for our purposes. Stace and Murrell[8] have studied collisional energy transfer for a variety of triatomic molecules in collisions with rare gas atoms. For the most part, their study concentrated on cases where the triatomic molecule had precisely the mean thermal energy based on the temperature of the bath gas. This is a rather special case and does not specifically address the question of the energy transfer properties of molecules within a few k_BT of the dissociation limit. That is, during the steady-state dissociation process, energy levels below a few k_BT less than the threshold energy have equilibrium populations. Consequently,

their energy transfer characteristics are not directly of interest.

In this paper we investigate the properties of He-HO_2 collisions in which the HO_2 is excited to energies near, but below, the dissociation limit. In a master equation formulation of the dissociation process the natural independent parameters are the two good constants of the motion of the isolated molecule, the total energy and total angular momentum, and the temperature of the heat bath. Therefore, we want particularly to determine how the collisional energy transfer properties depend on these variables. We have chosen to use the Melius-Blint[9] potential for HO_2, not so much because we believe it to be a perfect representation of the HO_2 surface, but because it is readily available, reasonable, and because we believe our results using it will be generally applicable to at least a class of small polyatomic molecules.

II. MATHEMATICAL MODEL

The methods of classical dynamics discussed by many investigators[10—17] are used in this study. The particular formalism used here incorporates five basic approximations: (1) the use of an analytical fit of an *ab initio* potential energy surface to describe the HO_2 molecule when separated from the He atom at infinity, (2) the use of three two body potentials to describe the He-HO_2 interaction, (3) the use of volume weighted orthant sampling, discussed in detail in our previous paper[10], to sample the phase space of the energized HO_2 molecule, (4) the use of Monte Carlo averaging techniques to sample the entire phase space of the He-HO_2 collision system, and (5) the treatment of the dynamics with classical mechanics.

A. The Potential Energy Surface

The potential energy surface used in this investigation is a function of six distances and can be written as

$$V = V_{HO_2}(R_1, R_2, R_3) + V_{He-HO_2}(R_4, R_5, R_6), \qquad (2.1)$$

where R_1 is the HO^1 distance, R_2 is the O^1-O^2 distance R_3 is the H-O^2 distance, R_4 is the He-H distance, R_5 is the He-O^1 distance, and R_6 is the He-O^2 distance. A schematic diagram of the He-HO_2 system is illustrated in Figure 1.

The V_{HO_2} surface is the analytical representation given by Melius and Blint[9] of their *ab initio* calculations. In this and our previous work[10] we have been interested in the intramolecular energy transfer and unimolecular reaction of HO_2 in the ground electronic $^2A''$ state. These processes are assumed to take place adiabatically. It is important to note the existence of a low- lying excited state surface of HO_2, the $^2A'$ state which correlates with excited state products $H(^2S) + O_2(^1\Delta_g)$ and lies approximately 17 kcal/mol above the ground state HO_2 surface in the region of configuration space. The choice of total system energies employed in this study (except for possible, yet highly improbable trajectories with anomalously high values of relative translational energy) rendered populating dissociative states on the excited-state surface highly improbable. The potential energy parameters that have been used in our study are given in Table I of our previous paper. The Melius-Blint calculations predict that the binding energy of HO_2 (referenced from $H + O_2$) is 44.2 kcal/mol compared to the experimentally determined value of 54 kcal/mol. Examination of the potential parameters also reveals the existence of a small exit barrier for dissociation of approximately 2 kcal/mol, which may be an artifact of the Melius-Blint calculations. Despite the aforementioned anomalies, the surface has been verified to be a reasonable representation of the potential energy of the HO_2 system, as discussed in our earlier paper.

The intermolecular potential V_{He-HO_2} is approximated as a sum of three two-body potentials as,

$$V_{He-HO_2} = V_{He-H}(R_4) + V_{He-O}(R_5) + V_{He-O}(R_6) \qquad (2.2)$$

In accord with Gallucci and Schatz[7], we have approximated the V_{He-H} potential as the He-He potential of Burgmans, et al[18] and the V_{He-O} potential as the He-Ne potential of Chen, et al.[19]

The approximation of the intermolecular potential energy as a summation of atom-atom pair potentials was also used by Suzukawa, et al[20] in their study of energy transfer in CO_2-rare gas systems. The pair potential approximation for the intermolecular potential is frequently invoked for lack of a more sophisticated surface, which in the four atom case involves three- and four-body interaction terms. The effect of the higher order terms for the O-H_2O system was investigated by Redmon, et al[21], who found that two-body potential terms can provide a correct zeroth order description of the interaction that is adequate for qualitative purposes.

B. Phase Space Sampling

The Monte Carlo averaging and volume weighted orthant sampling are performed in concert with one another to determine average collision characteristics for an ensemble of trajectories. For an ensemble of trajectories, we specify the translational temperature of the heat bath, the total internal molecular energy, and a range for the total molecular angular momentum. The notation $(T_t, E_m^i, J^l - J^h)$ is used to designate an ensemble. The symbol T_t designates the translational temperature in Kelvins, E_m^i the initial value of the molecular energy in kcal/mol, and J^l-J^h the range of molecular angular momentum from which the initial value is selected. The "spread" in designated J values is useful in enhancing the efficiency of the sampling process, since the J value is determined by a simple rejection procedure. The independent variables used here are those that naturally result from formulating the master equation for the dissociation of a polyatomic molecule, i.e., the two good constants of the motion for the isolated molecule and the temperature of the bath gas.

The initial step in the determination of the boundary conditions for each trajectory consists of randomly orienting the HO_2 molecule with respect to the incoming He atom. This is accomplished by first fixing the molecule at its equilibrium geometry with the origin at the molecular center-of-mass. The molecule is then rotated through three randomly chosen Euler angles to determine the position of the molecule in the space-fixed coordinate system. The four step volume weighted

orthant sampling technique, which is discussed in our earlier paper, is then employed to fix the the initial coordinates and momenta of the HO_2 for the prescribed value of E_m and J. The relative velocity for each trajectory is then selected randomly by Monte Carlo sampling the appropriate collision integral with an assumed Boltzmann distribution of velocities. Finally the impact parameter is selected from a b^2 distribution of values between 0 and b_{max}. Integration of several trajectories over the range of conditions utilized in our study revealed that a suitable value of the maximum impact parameter, b_{max}, was 4.0 Å. For trajectories fixed at $b = b_{max}$ = 4.0 Å, we found that the root mean squared energy transferred per collision did not greatly exceed the numerical error in integration of the equations of motion.

C. Classical Trajectory Calculations

Hamilton's equations are used to describe the time evolution of the system. The Hamiltonian for the system is written as

$$H(p_i, q_i) = \sum_{i=1}^{9} \frac{p_i^2}{2\mu_i} + V(R_1(q_i), R_2(q_i), R_3(q_i), R_4(q_i), R_5(q_i), R_6(q_i)) \qquad (2.3)$$

where the first three coordinates and conjugate momenta correspond to the Cartesian components of H relative to O^1, the second three correspond to the Cartesian components of O^2 relative to O^1 H, and the third three correspond to the Cartesian components of He relative to the center-of-mass of the HO_2 molecule. The relevent reduced masses are ($\mu_1 = \mu_2 = \mu_3 = \mu_{H,O^1}$), ($\mu_4 = \mu_5 = \mu_6 = \mu_{O^2,O^1H}$), and ($\mu_7 = \mu_8 = \mu_9 = \mu_{He-HO_2}$). The eighteen equations of motion derived from this Hamiltonian are integrated using the ordinary differential equation solver, ODE[22,23], written by Shampine and Gordon. Integration is initiated when the atom is separated from the molecular center-of-mass by 6.5 Å and is terminated when each of the atoms in the molecule is at least 6.5 Å from the He atom. Additional tests were made to check for the formation of Van der Waals complexes. No such trajectories were found. This is not surprising since the well depths for the He-H and He-O interaction potential are only 10 to 20 K (temperature units).

At the end of each trajectory, the energy and angular momentum distribu-

tions are determined. The final relative translational energy E_t^f in kcal/mol is computed and subtracted from the system total energy E_T to determine the final total molecular energy E_m^f,

$$E_m^f = E_T - E_t^f, \tag{2.4}$$

at the termination of the trajectory. The three components of the final molecular angular momentum are evaluated and used to determine the square of the final molecular angular momentum $(J^f)^2$, which is then used to evaluate the final "rotational" energy E_J^f as

$$E_J^f = B_{eff}(J^f)^2. \tag{2.5}$$

Strictly speaking, E_J is not the rotational energy, but is only part of it. However our purpose is not to make a rigorous separation between rotational and vibrational energy, but to distinguish between energy which can and cannot be used to dissociate the molecule. Total angular momentum is a constant of the motion in the isolated molecule and, in the language of RRKM theory, the energy associated with it, i.e. E_J, is frequently referred to as the centrifugal barrier. It is fixed and not available for redistribution within the molecule to promote unimolecular reaction. In general B_{eff} is a function of position along the reaction coordinate; however, in the present case, the difference between B_{eff} at the HO_2 equilibrium position and the transition state is so small that we have ignored it. The final molecular "vibrational" energy E'_f is determined from

$$E'_f = E_m^f - E_J^f. \tag{2.6}$$

This is consistent with the definition of rotational energy that we have adopted and represents the amount of energy in the molecule that is available for breaking the chemical bond. Consequently, the dissociation limit is defined approximately by the relation $E' = 46.3$ kcal/mol.

The final impact parameter is determined by computing the final orbital angular momentum $\overline{L}_o^f$ of the HO_2-He pair as the difference between the total system angular momentum $\overline{L}_T$ and the final molecular angular momentum $\overline{J}^f$. The impact

parameter is thus computed as

$$b = \left(\overline{L}_o^f \bullet \overline{L}_o^f\right)^{1/2} \mu_{HO_2-He} v_r^f, \tag{2.7}$$

where v_r^f is the magnitude of the final relative velocity vector. The scattering angle is determined by computing the angle between the initial and final relative velocity vectors.

The angular momenta important in this problem are the total angular momentum $\overline{L}_T$, the initial molecular angular momentum $\overline{J}^i$, the final molecular angular momentum $\overline{J}^f$ the initial orbital angular momentum $\overline{L}_o^i$, and the final orbital angular momentum $\overline{L}_o^f$. The magnitudes of these quantities are expressed as multiples of h throughout this work, i.e., they are dimensionless.

Energy transfer described in terms of changes in the total molecular energy, the relative translational energy, the rotational energy, and the vibrational energy are computed for each trajectory by subtracting relevant values of the initial energy from the final values. Angular momentum changes are determined in a similar fashion. Average values per collision (designated by a quantity enclosed in $<>$) of the changes in the molecular energy, the relative translational energy, the rotational energy, the vibrational energy, the molecular angular momentum, and the orbital angular momentum are computed for each ensemble of trajectories. Energy transfer distributions are also separated into activating and deactivating parts, the number of each kind of transition is determined, and a separate average is determined for the distribution. Subscripts a and d designate activating and deactivating transitions, respectively.

III. ENERGY TRANSFER CHARACTERISTICS

We have investigated energy transfer in HO_2-He collisions as a function of the initial translational temperature of the heat bath, the internal energy of the HO_2 molecule, and the angular momentum of the HO_2 molecule. These results are summarized in Table I. The three translational temperatures investigated are 800, 2000, and 5000 K. Initial values of the internal molecular energy are in the range 30 to 46 kcal/mol. The ranges of initial molecular angular momentum sampled are (0-10), for which the ensemble has an average value of approximately 7.5, (30-35), with an average value of 32.5, and (50-52), with an average value of 51. The average values of initial rotational energy associated with the three distributions of initial angular momenta are 0.17, 3.1,and 7.7 kcal/mol, respectively. The quantities tabulated are ensemble averages of the various types of energy transfer. The symbols nd and na indicate the number of vibrationally deactivating and activating trajectories, respectively, and their sum is the total number of trajectories for the ensemble.

There are some general energy transfer characteristics for this system that are important to mention. Less than 1/2 and frequently between 1/4 and 1/3 of all collisions are nearly elastic collisions with a scattering angle of approximatley zero. The magnitude of the average energy transferred per collision to the molecule is less than 1.6 kcal/mol. Average molecular angular momentum changes are less than 5 h, and average magnitudes of rotational energy transfer are less than a kcal/mol. The average vibrational transferred is generally negative and on the order of tenths of kcal/mol. The numbers of activating and deactivating trajectories are of similar value. The magnitude of the average vibrational energy transferred in activation and deactivation is in the range .17 to 1.9 kcal/mol with more energy, on the

average, transferred in deactivation.

Prior to comparing the energy transfer characteristics of the various ensembles to ascertain the effects of various distributions of energy and angular momentum, it is important to determine the precision of the averages. This is accomplished most easily through examination of the convergence of the average as a function of trajectory number. These data are displayed in Table II for the average total molecular energy transferred and for the average vibrational energy transferred per collision for sets of representative ensembles. Ensembles having a bath gas temperature of 800 K converge nicely at approximately 5000 trajectories with a precision of at least 0.05 kcal/mol. The precision of the averages for ensembles with a higher bath gas temperature is between 0.05 and 0.1 kcal/mol for 5000 trajectories. The width of the Boltzmann distribution at the higher temperature accounts for the somewhat smaller precision. A large number of trajectories, on the order of 5000, is normally required for the determination of the energy transfer averages (per collision). The relatively slow convergence results from the near cancellation of the combined effects of activating and deactivating collisions. In other words, the overall averages are determined by small difference between large numbers. As one might expect, the one-sided averages, i.e., activating or deactivating, converge somewhat more rapidly. In any event, none of our conclusions rely on any single average being precise to better than 0.1 kcal/mol.

Collisional energy transfer depends on three variables: the heat bath temperature, T_t, the total molecular energy, and the total molecular angular momentum. The dependence of energy transfer on these variables is complex. It is easier to understand if we introduce intensive variables that can be used to measure the degree of disequilibrium existing among the various degrees of freedom. This can be accomplished by introducing equivalent "temperatures" based on thermal equipartition of energies, i.e.

$$T_J = E_J/k_B \tag{3.1}$$

where

$$E_J = <J^2> B_{eff} \tag{3.2}$$

and

$$T_{E'} = (E')/(n + 1/2)k_B \tag{3.3}$$

where n = 3 is the number of vibrational degrees of freedom in the HO_2 molecule. The $(1/2\ k_B)$ term is contributed from rotation, and is associated with the rotational degree of freedom whose energy can be used to break the chemical bond. The three temperatures of the various ensembles are given in Table III.

Using Tables I and III, we see that energy transfer for the degree of freedom with the lowest of the three temperatures is always positive while that associated with the highest temperature is nearly always negative. When T_J is less than T_t and they differ by an order of magnitude, $<\Delta E_J>$ is positive and $<\Delta E_t>$ is negative. Generally the vibrational temperature is the highest of the three and $<\Delta E'>$ is negative.

One of the more interesting effects is determined from the comparision of ensembles for which T_t and E_m are constant and J^i is increased. For these ensembles, the effect of increasing J^i is to decrease $T_{E'}$ while increasing T_J. In going through such a progression, with a bath gas temperature of 800 K, we note that $<\Delta E_m>$, $<\Delta J>$, and $<\Delta E_J>$ decrease while $<\Delta E_t>$ increases. We also observe an increase in $-<\Delta E'>$ as long as $T_{E'}$ is greater than T_J. The increase in $-<\Delta E'>$ with increasing J^i results since $E' - t$ transfer is more efficient than the other modes of transfer. Increasing J^i tends to make the heat bath temperature the lowest temperature and increases the need for transfer to translation. This is accomplished most efficiently by transfer from vibration, thus producing the increase in $-<\Delta E'>$ with J^i. For the single case where the rotational temperature is greater than the vibrational temperature, $-<\Delta E_J>$ is greater than $-<\Delta E'>$. In going from an ensemble where the rotational temperature is lowest to one where it is highest, the energy transfer mechanism changes from transfer *to* rotation to transfer *from* rotation. At a bath gas temperature of 2000 K, the same trends in energy transfer with increasing J^i occur until the heat bath temperature becomes

the lowest temperature. Under these conditions, both internal degrees of freedom transfer energy to translation, and $-<E'>$ does not increase in changing J^i from (30-35) to (50-52). At a heat bath temperature of 5000 K, the effect of increasing J^i is somewhat different, since the translational and vibrational temperatures are comparable, and the rotational temperature is lowest. The quantity $<\Delta E_J>$ is positive and is not dependent on J^i. There is a slight tendency to transfer energy *from* the molecule at the lower J^i value, where the difference between the translational and vibrational temperature is greater, and to transfer energy *to* the molecule when the two temperatures are nearly equal. Although the average energy transferred per collision is very small, evidence for significant energy transfer is provided by the magnitudes of the averages associated with vibrationally activating and deactivating collisions, i.e. $<\Delta E'>_a$ and $-<\Delta E'>_d$. These both increase as J^i is increased; however the average energy transferred in vibrationally activating collisions increases more rapidly accounting for the small but positive value of $<\Delta E'>$ for $50 \leq J^i \leq 52$.

The importance of "temperature" in energy transfer is further illustrated by comparing ensembles that differ only in E_m^i. Increasing E_m^i for fixed T_t and J^i is equivalent to increasing $T_{E'}$ while holding T_t and T_J constant. If energy transfer between any two degrees of freedom were of equal probability, we should observe an increase in $-<\Delta E'>$ and an increase in energy transfer to the degree of freedom with the lowest temperature as vibrational temperature is increased. In general, this is the case; however, for ensembles where T_J is the lowest of the three temperatures, little change occurs in $-<\Delta E'>$ when $T_{E'}$ increases from 5430 to 6570 K, and $<\Delta E_J>$ does not change systematically. When T_t is the lowest temperature, we have $-<\Delta E'>$ and $<\Delta E_t>$ increasing as $T_{E'}$ increases. The effects noted from increasing $T_{E'}$ while holding other input variables fixed indicates that it is easier to transfer energy between translation and vibration than between rotation and vibration.

The effect of bath gas temperature can be determined by comparing ensembles that have the same values of initial molecular energy and angular momentum and

differ only in the initial value of bath gas temperature. The fraction of vibrationally activating collisions increases and the average amount of vibrational energy transferred in them increases with temperature. The increase in vibrational activation with temperature occurs because the Boltzmann distribution width increases with T_t and is shifted unsymmetrically toward higher values of translational energy.

Evidence has been noted above for all types of energy transfer. Further understanding of the energy transfer mechanisms is gained through the use of correlation coefficients, which provide a measure of the relationship between two energy transfer quantities on a single collision basis. Correlation coefficents are defined as

$$\alpha_{\gamma\beta} = \frac{\sum_{i=1}^{N} \frac{\Delta E_{\gamma i} \Delta E_{\beta i}}{N} - <\Delta E>_{\gamma} <\Delta E>_{\beta}}{S_{\gamma} S_{\beta}} \tag{3.4}$$

where S_γ represents the standard deviation of the quantity ΔE_γ in a distribution of N trajectories. Correlation coefficients assume values between -1.0 and $+1.0$. In the case of energy transfer, a negative value signifies that the loss of one quantity and gain of another are coupled in single collision events. The degree of coupling is indicated by the magnitude of the coefficient. Correlation coefficients were computed for the energy transfer between all pairs of the three degrees of freedom: translational, rotational, and vibrational, and are given in Table IV. Second moments of the energy transfer, some of which are used in computing the coefficients, are given in Table V. Coefficients of magnitude less than a 0.1 are regarded as zero, and all coefficients in excess of this amount are negative. In all cases, the correlation coefficient between translational and vibrational energy is largest in magnitude, indicating that the major mode of energy transfer is between the translational degrees of freedom and the vibrational degrees of freedom in the molecule. This may lead to the incorrect conclusion that the average vibrational energy transferred per collision should be the largest of the overall averages for the various ensembles, which is not true. It implies instead that the most prevalent transfer mechanism is between translation and vibration, and when activation and deactivation are considered, it is easy to reconcile that a significant amount of energy transfer can yield a small $<\Delta E'>$ per collision. For most ensembles, the correlation coefficients indicate

reasonable amounts of $E' - t$ and $t - J$ energy exchange.

Additional understanding of the the effect of increasing initial angular momentum for ensembles having a fixed heat bath temperature and initial molecular energy is gained by examining the correlation coefficients. At a heat bath temperature of 800 K we observe a change in the energy transfer mechanism with increasing J^i, from positive to negative $<\Delta E_J>$. As J^i is increased, we see a decline in the $J - E'$ correlation coefficent and an increase in the $t - J$ coefficient. The rotational energy transfer mechanism shifts from predominantly $E' - J$ transfer to predominantly $J - t$ transfer. The most profound effect of increasing J^i is to increase the tendency for transfer to translation, and this usually occurs from E' since E' to t transfer is the most efficient mode. The amount of vibrational-rotational energy exchange at the *largest* J^i depends on the relative magnitudes of the temperatures associated with the two degrees of freedom. For this case, if $T_J < T_{E'}$, there is almost no $J - E'$ transfer. In the opposite case where $T_J > T_{E'}$ there there is a small amount of $J - E'$ transfer. At 2000 K, the same type of energy transfer mechanism as observed at 800 K prevails. Under the condition $T_J \approx T_t$, little $t - J$ transfer occurs. At 5000 K, the correlation coefficients indicate that rotational energy transfer is almost exclusively from translation until $T_{E'}$ and T_t become similar in value.

The very low J cases at 800K illustrate a very interesting feature. In these cases the dominant vibrational deactivation mechanism is collision induced intramolecular $E' - J$ transfer. This conclusion is most readily drawn from the results $-<\Delta E'> \approx -<\Delta E_J>$ and $\alpha_{tJ} \approx 0$. Since there is no $t - J$ correlation, the rotational energy gain must come directly from vibration. Under these conditions the most effective type of collision is one in which angular momentum is transferred to the molecule, with little or no transfer of energy. In general, transferring angular momentum involves changes both in the impact parameter and the relative velocity. This is probably why these low J cases normally have very small losses of relative translational energy.

The use of correlation coefficients and equivalent temperatures is useful in

understanding the energy trasnfer mechanism. However, it is also important not to lose sight of the major results of the trajectory calculations:

1. At fixed T_t and E', $-<\Delta E'>$ and $-<\Delta E>_d$ always increase with increasing J (see Fig. 2). For cases very close to the dissociation limit, this statement is true even at fixed E_m.

2. At fixed J and E', $-<\Delta E'>$ decreases with increasing translational temperature (see Fig. 3). This is primarily a "thermodynamic" effect in which $<\Delta E'>_d$ remains relatively constant, and $<\Delta E'>_a$ and the fraction of activating collisions increase.

3. At very low J, $<\Delta E'>$ is independent of E' (or E_m), whereas at higher J, $<\Delta E'>$ is a strong function of E' (see Fig. 2). These changes in $<\Delta E'>$ are due primarily to changes in $<\Delta E'>_d$.

IV. ENERGY TRANSFER CROSS SECTIONS

In the evaluation of the low pressure limit unimolecular rate coefficient it is desirable to express the energy transfer characteristics of a system undergoing unimolecular decay in the form of transition probabilities or energy transfer cross sections. Cross sections cannot be computed in a classical calculation without the assignment of a cut-off impact parameter. The value of $b_{max} = 4.0$ Å was determined from the criterion that no trajectories lead to sizable energy transfer for b $> b_{max}$. Although the collisional averages of energy transfer depend on the value of b_{max}, energy transfer cross sections do not, providing, of course, that the maximum impact parameter has been selected in a reasonable manner. Stace and Murrell[8] have discussed at length the choice of b_{max} and have used the criterion that b_{max} should be chosen such that $|<\Delta E>|/k_BT$ is less than 0.05. They also

indicate that the choice of b_{max} can also be based upon the scattering angle. In their calculations, their selected values of b_{max} yielded scattering angles less than three degrees. In our own calculations the choice of b_{max} was comparable to values selected by Stace and Murrell for similar systems and yielded nearly zero values of scattering angle. For trajectories fixed at b = b_{max}, we found that the root mean squared energy transferred per collision did not greatly exceed the numerical error in the integration of the equations of motion.

The "shape" of the vibrational energy transfer function, i.e. the dependence of the cross section $\delta\sigma(T_t, E', J, \Delta E')$ on $\Delta E'$, is of particular interest. The function $\delta\sigma(T_t, E', J, \Delta E')$ is defined by the relation,

$$\delta\sigma = \frac{d\sigma}{dE'_f}\delta E'_f \tag{4.1}$$

where $\delta E'_f$ is a bin width. Although considerable evidence has been given[1] that low pressure limit, thermal, single channel, unimolecular reactions are insensitive to this function, such may not be the case under other experimental conditions. Multi-channel thermal reactions, or photo- or chemically-activated reactions, may be quite sensitive to this function under certain conditions. Therefore, we have examined the $\delta\sigma(T_t, E', J, \Delta E')$ functions resulting from our trajectory calculations. The functional form for the activating and deactivating vibrational energy transfer cross sections that we find most satisfactory is

$$\delta\sigma(T_t, E', J, \Delta E') = B_1\exp(-|\Delta E'|/B_2) + B_3\exp(-|\Delta E'|/B_4). \tag{4.2}$$

The fitting coefficients B_1 through B_4 are given in Table VI for the vibrationally deactivating collisions and in Table VII for the vibrationally activating collisions. The $\Delta E' = 0$ bin is always neglected when fitting the histograms to Eq. (4.2). This is the only bin whose cross section depends on the assumed value of b_{max} providing that b_{max} was large enough to begin with. If b_{max} is then increased, $\delta\sigma(T_t, E', J, 0)$ will increase, but other cross sections remain fixed. Consequently, the cross sections we have determined are *independent of the maximum impact parameter.*

Figures 4 through 7 contain histograms of $\delta\sigma(T_t, E', J, \Delta E')$ for representative cases. The bold lines indicate the analytical fit to the cross section given by Eq.(4.2). Clearly, neither $\delta\sigma_d(T_t, E', J', \Delta E')$ nor $\delta\sigma_a(T_t, E', J, \Delta E')$ is well represented by a simple exponential function, the functional form most commonly assumed. In particular, the histograms show the significant high energy tails of the energy transfer distributions.

Tables VI and VII indicate that the B_1 and B_2 coefficients, which are more sensitive to the low energy transfer collisions, do not vary greatly with translational temperature, initial molecular energy, initial angular momentum and certainly not in any systematic manner. In contrast, the B_3 and B_4 coefficients vary by factors of two, indicating that the high energy tails are more sensitive to the initial energy and angular momentum distributions. The near constancy of B_1 and B_2 and the variation in B_3 and B_4 suggest that the average vibrational energy transferred per collision is dominated by the longer range portion of the distributions. A good measure of the relative importance of "weak" and "strong" collisions is provided by the ratio of the integrals of the two different terms, equal to (B_1B_2/B_3B_4). The ratio, (B_1B_2/B_3B_4), has values in the range 0.7 to 2.0 for vibrational deactivation, and is in the range .8 to 4.2 for vibrational activation. Large values of the ratio occur when $J - E'$ transfer is important, indicating that this occurs via weak collisions. The smallest values of the ratio for both activation and deactivation occur for the last three entries in each table: (2000,46,50-52), (5000,46,30-35), and (5000,46,50-52), where the high energy tails are quite pronounced.

The average vibrational energy transferred per collision in weak collisions is proportional to $B_1(B_2)^2$, and in strong collisions it is proportional $B_3(B_4)^2$. The ratio, $(B_1B_2^2/B_3B_4^2)$ is in the range .04 to .20 for vibrational deactivation, and in the range .05 to .50 for vibrational activation. In general, the high energy tail has greater relative importance in deactivation than activation. At 5000 K the strong collision parameters for activation and deactivation are approximately equal. This behavior is exactly that which would be expected from microscopic reversibility,i.e., the relative importance of activation increases with temperature until activation and

deactivation play comparable roles in vibrational energy transfer. For ensembles at 5000 K, we begin to approach the conditions where the activating and deactivating energy transfer distributions are of similar shape, strong collisions play more important roles in each, and the net average vibrational energy transfer is nearly zero due to cancellation of nearly equal but opposite contributions to the average. Figure 4 illustrates the dependence of the vibrational deactivation cross section on $\Delta E'$ for the ensemble (2000,46,0-10), and is typical of cases where strong collisions are of minor importance. Figure 5 is a similar plot for the ensemble (5000,46,50-52), and illustrates cases where strong collisions play a major role in vibrational deactivation. Figure 6 is a plot of the vibrational activation cross section as a function of energy transferred for the ensemble (800,30,30-35) and exhibits the rather fast fall-off at small $\Delta E'$, which is typical of rather weak activation. Figure 7 for the ensemble (5000,46,50-52), is typical of activation dominated by strong collisions. The shapes of Figures 5 and 7 are nearly identical.

Further information on the energy transfer distributions can be determined from the standard deviations of the average energy tranfer quantities, which provide a useful measure of the spread or distribution width. Standard deviations for the quantities, $<\Delta E_m>$, $<\Delta E'>$, and $<\Delta E'>_d$, are given in Table VIII. In general the standard deviations are functions of the three variables T_t, E_m, and J^i. As T_t is increased, the standard deviation for vibrational activation increases. At 800 and 2000 K, the standard deviation for vibrational deactivation is greater than for activation, and at 5000 K they are comparable. The smallest standard deviations are observed for bath gas temperatures of 800 K and $J^i < 10$, where strong collisions play a minor role.

Figures 8 through 11 are three-dimensional histograms for combined rotational -vibrational energy transfer. Many of the points we have discussed above can be seen qualitatively from these figures. Note, however, that the bin centered at the origin has been cut off in each case to maintain definition of the figure. The cross section functions defined by these histograms are precisely those which enter the two-dimensional master equation formulation for the thermal rate coefficient.

V. THE TOTAL VIBRATIONAL ENERGY TRANSFER CROSS SECTION AND CORRECTED VALUES OF $<\Delta E'>$

It is possible from the $\Delta E'$ histograms to determine unambiguous values of the total vibrational energy transfer cross sections $\sigma_{E'}(T_t, E', J)$ and corrected values of $<\Delta E'>$, $<\Delta E'>_c$, that are *independent* of b_{max}. The general definition of $\sigma(T_t, E', J)$ is

$$\sigma_{E'}(T_t, E', J) = \int_0^\infty \frac{d\sigma(T_t, E', J, E'_f)}{dE'_f} dE'_f, \tag{5.1}$$

where $d\sigma(T_t, E', J, E'_f)/dE'_f$ is the function defined in Eqs. (4.1) and (4.2). The function $d\sigma(T_t, E', J, E'_f)/dE'_f$ is related to the total vibrational energy transfer rate constant $Z_{E'}(T_t, E', J)^{(1)}$ by the relation

$$Z_{E'}(T_t, E', J) = \sqrt{\frac{8k_B T_t}{\pi \mu_{He-HO_2}}} n_{He} \sigma_{E'}(T_t, E', J). \tag{5.2}$$

The calculation of $\sigma_{E'}$ is most easily accomplished by removing the "anomalous collisions" from the $\Delta E' = 0$ bin of the histograms. The fraction of anomalous collisions in any sample is simply

$$\frac{N(0)}{N_T} - \frac{B_1 + B_3}{\pi b_{max}^2} \tag{5.3}$$

where $N(0)/N_T$ is the fraction of trajectories in the $\Delta E' = 0$ bin. The term $(B_1 + B_3/\pi b_{max}^2)$ is the fraction of "good collisions" in the $\Delta E' = 0$ bin. In practice we evaluate B_1 and B_3 from the deactivation fits, rather than those for activation; however, in principle either can be used. It follows immediately that $\sigma_{E'}/\pi b_{max}^2$ is given by

$$\frac{\sigma_{E'}(T_t, E', J)}{\pi b_{max}^2} = 1 - \left[\frac{N(0)}{N_T} - \frac{B_1 + B_3}{\pi b_{max}^2}\right] \tag{5.4}$$

Values of $\sigma_{E'}(T_t, E', J)$ are tabulated in Table IX. In general, $\sigma_{E'}$ does not vary greatly as a function of T_t, E', and J, and with good precision we can say that $\sigma_{E'}/\pi b_{max}^2 \approx 0.7 \pm 20$ for all cases considered. By completely identical reasoning we can correct $<\Delta E'>$ to the new definition of a collision. The correction is

$$<E'>_c = \frac{\pi b_{max}^2}{\sigma_{E'}} <\Delta E'> \tag{5.5}$$

for any ensemble of trajectories. The correction factor is the same for any moment of the full vibrational energy transfer probability density function. Note that

$$Z_{bmax} <\Delta E'> = Z_{E'} <\Delta E'>_c \tag{5.6}$$

i.e. the vibrational energy transferred per unit time per molecule in a given state is independent of the "definition" of a collision.

The procedure introduced in the previous paragraph is a reasonable method for removing the singularity at $E'_f = E'_i$ that exists in the integral (5.1). This singularity occurs only in classical mechanics, not in quantum mechanics. It is a direct consequence of very large impact parameter collisions and is related to the singularity at zero scattering angle in the classical differential scattering cross section.

From the values of $\sigma_{E'}$ in Table IX we can deduce optimum values of the maximum impact parameter to be used in classical trajectory calculations for each case. The optimum values of b_{max} for the cases considered here range from 3.0 $\AA$ to 3.7 $\AA$. However,it appears to be a good idea in practice to choose b_{max} somewhat larger than the optimum value.

Values of $\sigma_{E'}$ obtained from Table IX are approximately 35 $\AA^2$, whereas the Lennard-Jones cross section at 800K,

$$\sigma_{LJ} = \pi l_{LJ}^2 \Omega^{(2,2)*}, \tag{5.7}$$

is 28.3 $\AA^2 (\sigma_{LJ}/\pi b_{max}^2 = 0.56)$. Due to the drop of $\Omega^{(2,2)*}$ with increased temperature,σ_{LJ} is even smaller at higher temperatures. Although the values of $\sigma_{E'}$ in

Table IX are systematically larger than σ_{LJ}, the use of σ_{LJ} in the calculation of unimolecular rate coefficients probably does not lead to unacceptable error in most cases. This conclusion is in agreement with that of Troe[3], based on the trajectory calculations of Stace and Murrell. However, it is important to point out that Troe's definition of σ_{LJ} incorrectly excludes the factor π in Eq. (5.7). When Troe compares σ_{LJ} with b_{max} values, he also incorrectly excludes a factor of π in πb_{max}^2, so that the relative comparison is correct. The practice of excluding the π in σ_{LJ} appears to have originated in unimolecular rate studies of relative efficiencies of different colliders. In such an application the constant factor of π is unimportant, but in computing the absolute values of unimolecular rate coefficients, it must be included.

It is also possible to estimate $\beta_{c\Delta E'}$, the weak collision correction factor to the strong collision rate coefficient, from the trajectory calculations. If one follows Troe's development closely, it is easy to deduce that $\beta_{c\Delta E'}$ can be computed from the expression

$$\frac{\beta_{c\Delta E'}}{1-\sqrt{\beta_{c\Delta E'}}} = -\frac{<\Delta E'>_c}{F_E k_B T}, \tag{5.8}$$

where $F_E \approx 1$ and, as indicated, it is the corrected average $<\Delta E'>_c$ that is to be used in Eq. (5.8). We can estimate the temperature dependence of $\beta_{c\Delta E'}$ from $<\Delta E'>$ values taken from Table I, correction factors from Table IX, and Eq. (5.8). The following table is obtained:

T_t	$\beta_{c\Delta E'}$
$800K$	~ 0.25
$2000K$	~ 0.15
$5000K$	<0.01

These values of $\beta_{c\Delta E'}$ are reasonably representative of those deduced experimentally for similar unimolecular dissociations. A direct comparison of our trajectory results with experimental data for HO_2 is beyond the scope of this investigation.

The very low value of $\beta_{c\Delta E'}$ obtained at $T_t = 5000K$ is a very interesting result. It is a direct consequence of the temperature T_t rising to the point where the mean thermal vibrational energy in the molecule at T_t approaches within a few $k_B T_t$ of the dissociation limit. In such a case the fraction of activating collisions and $<\Delta E'>_a$ increase to the point where $<\Delta E'>$ approaches zero. The effect is clearly overestimated here, since the mean thermal vibrational energy at T_t in any real molecule is always less than the classical equipartition energy $[(n + 1/2)k_B T]$. Nevertheless, the effect should exist qualitatively in real molecules. It should be most pronounced in larger molecules with relatively weak bonds. Examples that immediately come to mind of molecules whose dissociations may show very low values of β_c for this reason include C_2H_5, C_2H_3, HCO, and NNH.

SUMMARY AND CONCLUSIONS

We have used classical trajectories to compute the energy transfer properties of HO_2 molecules (Melius-Blint surface) excited to energies near the dissociation limit in collisions with helium. In general, the average "vibrational" energy transferred per collision is a function of all three parameters considered: heat bath temperature, total molecular energy, and total molecular angular momentum. The most important effects can be summarized as follows:

1. At fixed vibrational energy and heat bath temperature, $-<\Delta E'>$ increases markedly with increased molecular angular momentum J. This statement is true even at fixed total molecular energy if we restrict ourselves to energies close to the dissociation limit.

2. For fixed J and heat bath temperature T_t, $-<\Delta E'>$ increases as E_m increases *except* for very low J cases. For the low J cases $<\Delta E'>$ is very small and is essentially independent of E_m or E'.

3. The magnitude of the average vibrational energy transferred per collision decreases as T_t is increased. This is principally a "thermodynamic" effect in which $<\Delta E'>_a$ and the fraction of activating collisions increase rapidly with T_t. The contribution from deactivation remains relatively constant.

4. Two mechanisms are important in vibrationally deactivating the molecule. At low J and low T_t, deactivation occurs primarily by collisions that simply rearrange the energy in the molecule, converting "vibrational" energy to "rotational" energy. At higher J and T_t, translational-vibrational exchange is dominant.

The vibrational energy transfer cross section function,$\delta\sigma$, is not well represented by a simple exponential. Both the deactivating and activating parts have high energy tails, and each must be represented by the sum of two exponential functions. The high energy and low energy exponentials are of comparable importance in determining moments of the distribution function. Most of the variations in the average properties discussed above are consequences of changes in the "high energy" exponentials, i.e. in the tails of the distributions.

We have determined total vibrational energy transfer cross sections by removing the singularity in its derivative at $\Delta E' = 0$. These cross sections are relatively weak functions of E_m, T_t, and J and are somewhat larger than the Lennard-Jones cross sections.

ACKNOWLEDGMENTS

This work was supported in part by the Director, Office of Energy Research, Office of Basic Energy Sciences, Chemical Sciences Division of the U.S. Department of Energy, under Contract No. DE-AC03-76F00098; and in part, by Sandia National Laboratories for the Department of Energy under Contract DE-AC04-76DP00789.

We are grateful to Ms. Fran Rupley for her help with the computer graphics.

REFERENCES

1. J. Troe *J. Chem. Phys.* **66**, 4745 (1977).
2. J. Troe, *J. Chem. Phys.* **66**, 4758 (1977).
3. J. Troe, *J. Phys. Chem.* **83**, 114 (1979).
4. J. Troe, *J. Chem. Phys.* **77**, 3485 (1982).
5. J. Troe, *Ber. Bunsenges. Pys. Chem.* **87**, 161 (1983).
6. R. G. Gilbert, K. Luther, and J. Troe, *Ber. Bunsenges. Phys. Chem.* **87**, 169 (1983).
7. C.R. Gallucci and G. C. Schatz, *J. Phys. Chem.* **86**, 114 (1979).
8. A. J. Stace and J. N. Murrell, *J. Chem. Phys.* **68**, 3028 (1978).
9. C.F. Melius and R. J. Blint, *J. Chem. Phys. Let.* **64**, 183 (1979).
10. J. A. Miller and N. J. Brown, *J. Phys. Chem.* **86**, 772 (1982).
11. D.L. Bunker, *J. Chem. Phys.* **37**, 393 (1962).
12. D.L. Bunker, *J. Chem. Phys.* **40**, 1946 (1964).
13. D.L. Bunker and W. L. Hase, *J. Chem. Phys.* **59**, 4621 (1973).
14).. R.J. Wolf and W. L. Hase, *J. Chem. Phys.* **72**, 316 (1980).
15. N.J. Brown and D.M. Silver, *J. Chem. Phys.* **65**, 311 (1976).
16. J.A. Miller, *J. Chem. Phys.* **74**, 5120 (1981).
17. J.A. Miller, *J. Chem. Phys.* **75**, 5349 (1981).
18. A.L. Burgmans, J.M. Farrar, and Y.T. Lee, *J. Phys. Chem.* **64**, 1345 (1976).
19. C.H. Chen, P.E. Siska, and Y.T. Lee, *J. Phys. Chem.* **59**, 601 (1973).
20. H.H. Suzakawa, M. Wolfsberg, and D.L. Thompson, *J. Chem. Phys,*. 68, 455 (1975).
21. M.J. Redmon, R. J. Bartlett, B.C. Garrett, G.D. Purvis, P.M. Saatzer, G.C. Schatz, and I. Shavitt, in *Potential Energy Surfaces and Dynamics Calculations*, D.G. Truhlar, ed., Plenum, New York, p. 771 (1981).

22. T.H. Jefferson, Sandia National Laboratories Report SAND77-8274, Livermore, CA. (1977).

23. L.F. Shampine and M.K. Gordon *Computer Solutions of Ordinary Differential Equations: The Initial Value Problem*, W. H. Freeman, San Francisco, CA. (1975).

LIST OF TABLES

FIGURE CAPTIONS

1. Schematic diagram defining the interatomic coordinates R_1 through R_6.

2. Plots of the average vibrational energy transferred per collision as a function of vibrational energy at $T_t = 800$K. The straight lines drawn between the points are for clarity, not to indicate the actual functional dependence.

3. Plots of the average vibrational energy transferred per collision as a function of T_t. The straight lines drawn between the points are for clarity, not to indicate the actual functional dependence.

4. Histogram of the vibrational deactivation energy transfer cross section as a function of energy transfer for the ensemble (2000,46,0-10). Bold line in figure indicates fitted value of $\delta\sigma(T_t, E', J, \Delta E')$.

5. Histogram of the vibrational deactivation energy transfer cross section as a function of energy transfer for the ensemble (5000,46,50-52). Bold line in figure indicates fitted value of $\delta\sigma(T_t, E', J, \Delta E')$.

6. Histogram of the vibrational activation energy transfer cross section as a function of energy transfer for the ensemble (800,30,30-35). Bold line in figure indicates fitted value of $\delta\sigma(T_t, E', J, \Delta E')$.

7. Histogram of the vibrational activation energy transfer cross section as a function of energy transfer for the ensemble (5000,46,50-52). Bold line in figure indicates fitted value of $\delta\sigma(T_t, E', J, \Delta E')$.

8. Three-dimensional histograms of $\delta\sigma(T_t, E', J, \Delta E_J, \Delta E')$ as a function of ΔE_J and $\Delta E'$ for the ensemble (800,46,0-10).

9. Three-dimensional histograms of $\delta\sigma(T_t, E', J, \Delta E_J, \Delta E')$ as a function of ΔE_J and $\Delta E'$ for the ensemble (800,30,30-35).

10. Three-dimensional histograms of $\delta\sigma(T_t, E', J, \Delta E_J, \Delta E')$ as a function of ΔE_J and $\Delta E'$ for the ensemble (800,46,50-52).

11. Three-dimensional histograms of $\delta\sigma(T_t, E', J, \Delta E_J, \Delta E')$ as a function of ΔE_J and $\Delta E'$ for the ensemble (5000,46,50-52).

TABLE I

T_t	E_m^i	J^i	$\langle \Delta E_m \rangle$	$\langle \Delta J \rangle$	$\langle \Delta E_t \rangle$	$\langle \Delta E_J \rangle$	$\langle \Delta E' \rangle$	nd	$\langle \Delta E' \rangle_d$	na	$\langle \Delta E' \rangle_a$
800	30	0-10	7.2×10^{-2}	2.4	-7.2×10^{-2}	1.8×10^{-1}	-1.1×10^{-1}	2317	-4.3×10^{-1}	2183	2.3×10^{-1}
800	38	0-10	1.2×10^{-1}	3.3	-1.2×10^{-1}	2.5×10^{-1}	-1.3×10^{-1}	2306	-5.1×10^{-1}	2194	2.6×10^{-1}
800	46	0-10	2.6×10^{-3}	1.7	-2.9×10^{-3}	1.3×10^{-1}	-1.3×10^{-1}	4869	-4.9×10^{-1}	5381	2.1×10^{-1}
800	30	30-35	-2.9×10^{-1}	-4.3×10^{-1}	2.9×10^{-1}	1.3×10^{-3}	-3.0×10^{-1}	5048	-7.6×10^{-1}	4952	1.7×10^{-1}
800	41	30-35	-3.6×10^{-1}	-1.5×10^{-1}	3.6×10^{-1}	5.2×10^{-2}	-4.1×10^{-1}	2267	-1.1	2233	2.4×10^{-1}
800	46	30-35	-5.1×10^{-1}	-3.5×10^{-1}	5.1×10^{-1}	2.0×10^{-2}	-5.3×10^{-1}	2405	-1.2	2095	2.7×10^{-1}
800	30	50-52	-6.8×10^{-1}	-1.8	6.8×10^{-1}	-4.2×10^{-1}	-2.5×10^{-1}	2553	-9.7×10^{-1}	2447	4.9×10^{-1}
800	46	50-52	-1.2	-2.2	1.2	-5.1×10^{-1}	-7.2×10^{-1}	2662	1.9	2338	6.1×10^{-1}
2000	46	0-10	2.4×10^{-1}	2.7	-2.4×10^{-1}	2.4×10^{-1}	-1.1×10^{-3}	4500	-4.5×10^{-1}	5000	4.0×10^{-1}
2000	46	30-35	-3.5×10^{-1}	2.0×10^{-1}	3.5×10^{-1}	1.6×10^{-1}	-5.0×10^{-1}	2273	-1.5	2227	4.8×10^{-1}
2000	46	50-52	-1.5	-4.2	1.5	-9.8×10^{-1}	-4.8×10^{-1}	2553	-1.9	2447	1.0
5000	46	30-35	-3.1×10^{-2}	-6.7×10^{-1}	3.0×10^{-2}	3.2×10^{-2}	-6.4×10^{-2}	2267	-1.4	2733	1.0
5000	46	50-52	7.6×10^{-2}	-4.3×10^{-1}	-7.6×10^{-2}	3.5×10^{-2}	4.1×10^{-2}	4817	-1.5	5183	1.5

TABLE II

Number	(800,46,0-10) $\langle\Delta E_m\rangle$	(800,46,0-10) $\langle\Delta E'\rangle$	(800,30,30-35) $\langle\Delta E_m\rangle$	(800,30,30-35) $\langle\Delta E'\rangle$	(800,41,30-35) $\langle\Delta E_m\rangle$	(800,41,30-35) $\langle\Delta E'\rangle$	(800,46,50-52) $\langle\Delta E_m\rangle$	(800,46,50-52) $\langle\Delta E'\rangle$	(2000,46,30-35) $\langle\Delta E_m\rangle$	(2000,46,30-35) $\langle\Delta E'\rangle$	(5000,46,50-52) $\langle\Delta E_m\rangle$	(5000,46,50-52) $\langle\Delta E'\rangle$
1000	-1.3×10^{-2}	-1.2×10^{-1}	-3.1×10^{-1}	-2.3×10^{-1}	-3.7×10^{-1}	-4.4×10^{-1}	-1.2	-6.6×10^{-1}	-5.4×10^{-1}	-5.4×10^{-1}	-1.5×10^{-1}	-3.7×10^{-2}
2000	-1.1×10^{-2}	-1.3×10^{-1}	-3.2×10^{-1}	-2.2×10^{-1}	-3.3×10^{-1}	-3.9×10^{-1}	-1.2	-6.4×10^{-1}	-4.8×10^{-1}	-4.8×10^{-1}	-3.2×10^{-2}	1.8×10^{-2}
3000	-2.0×10^{-2}	-1.4×10^{-1}	-3.4×10^{-1}	-2.2×10^{-1}	-3.2×10^{-1}	-3.9×10^{-1}	-1.3	-7.1×10^{-1}	-4.3×10^{-1}	-4.2×10^{-1}	2.4×10^{-2}	6.1×10^{-2}
4000	-2.5×10^{-2}	-1.4×10^{-1}	-3.4×10^{-1}	-2.3×10^{-1}	-3.6×10^{-1}	-4.1×10^{-1}	-1.2	-6.8×10^{-1}	-3.7×10^{-1}	-5.0×10^{-1}	6.5×10^{-2}	6.7×10^{-2}
4500	-2.7×10^{-2}	-1.5×10^{-1}			-3.6×10^{-1}	-4.1×10^{-1}			-3.5×10^{-1}	-5.0×10^{-1}		
5000			-3.3×10^{-1}	-2.4×10^{-1}			-1.2	-7.2×10^{-1}			6.5×10^{-2}	7.0×10^{-2}
6000			-3.2×10^{-1}	-2.6×10^{-1}							3.8×10^{-2}	3.3×10^{-2}
7000			-3.2×10^{-1}	-2.7×10^{-1}							3.2×10^{-2}	1.7×10^{-2}
8000			-3.0×10^{-1}	-2.8×10^{-1}							5.3×10^{-2}	1.6×10^{-2}
9000			-3.0×10^{-1}	-2.9×10^{-1}							7.7×10^{-2}	3.1×10^{-2}
10000			-2.9×10^{-1}	-3.0×10^{-1}							7.6×10^{-2}	4.1×10^{-2}
10250	$+2.6\times10^{-3}$	-1.3×10^{-1}										

TABLE III

T_t	E_m^i	J^i	$T_{E'}$	T_J
800	30	0-10	4290	85
800	38	0-10	5430	85
800	46	0-10	6570	85
800	30	30-35	3830	1600
800	41	30-35	5400	1600
800	46	30-35	6110	1600
800	30	50-52	3200	3800
800	46	50-52	5490	3800
2000	46	0-10	6570	85
2000	46	30-35	6110	1600
2000	46	50-52	5490	3800
5000	46	30-35	6110	1600
5000	46	50-52	5490	3800

TABLE IV

T_t	E_m^i	J^i	α_{tJ}	$\alpha_{tE'}$	$\alpha_{JE'}$
800	46	0-10	+.06	-.91	-.46
800	30	30-35	-.33	-.70	-.44
800	41	30-35	-.06	-.83	-.51
800	46	30-35	-.21	-.87	-.29
800	30	50-52	-.61	-.66	-.18
800	46	50-52	-.51	-.84	-.03
2000	46	0-10	-.52	-.76	-.17
2000	46	30-35	-.13	-.85	-.41
2000	46	50-52	-.60	-.84	+.06
5000	46	30-35	-.38	-.90	-.06
5000	46	50-52	-.35	-.83	-.24

TABLE V

T_t	E'_m	J'	$\langle \Delta E_m^2 \rangle$	$\langle \Delta E'^2 \rangle$	$\langle \Delta E_t \Delta E_J \rangle$	$\langle \Delta E_t \Delta E' \rangle$	$\langle \Delta E_J \Delta E' \rangle$
800	46	0-10	1.5×10^{-1}	1.5×10^{-1}	$+2.2 \times 10^{-2}$	-7.5×10^{-1}	-1.9×10^{-1}
800	30	30-35	4.1×10^{-1}	2.2×10^{-1}	-4.8×10^{-1}	-1.4	-6.6×10^{-1}
800	41	30-35	5.3×10^{-1}	4.3×10^{-1}	-8.7×10^{-2}	-2.7	-1.1
800	46	30-35	7.6×10^{-1}	6.1×10^{-1}	-4.6×10^{-1}	-4.2	-6.6×10^{-1}
800	30	50-52	1.1	5.5×10^{-1}	-2.2	-2.3	-3.5×10^{-1}
800	46	50-52	2.5	1.7	-3.8	-9.2	$+1.8 \times 10^{-1}$
2000	46	0-10	1.6×10^{-1}	1.1×10^{-1}	-3.5×10^{-1}	-5.9×10^{-1}	-9.8×10^{-2}
2000	46	30-35	1.1	9.6×10^{-1}	-4.0×10^{-1}	-5.6	-1.6
2000	46	50-52	4.0	2.2	-6.6	-11.3	$+9.0 \times 10^{-1}$
5000	46	30-35	2.0	1.4	-2.0	-10.0	-3.2×10^{-1}
5000	46	50-52	2.7	2.1	-2.9	-11.4	-1.9

TABLE VI

T_t	E_m^i	J^i	$B_1(\text{Å}^2)$	B_2(kcal/mol)	$B_3(\text{Å}^2)$	B_4(kcal/mol)
800	46	0-10	6.4	.17	.32	1.7
800	30	30-35	6.4	.15	.26	2.4
800	41	30-35	6.4	.16	.33	2.6
800	46	30-35	5.9	.17	.26	2.8
800	30	50-52	4.9	.19	.41	2.3
800	46	50-52	5.0	.19	.36	3.2
2000	46	0-10	4.6	.18	.48	1.3
2000	46	30-35	4.6	.19	.27	3.1
2000	46	50-52	4.0	.18	.33	3.3
5000	46	30-35	3.3	.18	.40	2.2
5000	46	50-52	3.0	.21	.33	2.8

TABLE VII

T_t	E^i_m	J^i	B_1 (A^2)	B_2 (kcal/mol)	B_3 (A^2)	B_4 (kcal/mol)
800	46	0-10	5.1	.16	.58	.89
800	30	30-35	7.6	.14	.29	.89
800	41	30-35	7.0	.15	.49	.86
800	46	30-35	7.0	.12	.86	.78
800	30	50-52	6.3	.17	.42	1.5
800	46	50-52	6.6	.16	.55	1.6
2000	46	0-10	4.3	.17	.46	1.1
2000	46	30-35	4.7	.16	.55	1.2
2000	46	50-52	6.3	.13	.47	2.2
5000	46	30-35	3.9	.17	.40	2.1
5000	46	50-52	3.4	.20	.31	2.7

TABLE VIII

T_t	E_m^i	J^i	$S_{\Delta E_m}$	$S_{\Delta E'}$	$S_{\Delta E'_d}$	$S_{\Delta E'_a}$
800	30	0-10	7.9×10^{-1}	7.4×10^{-1}	8.0×10^{-1}	5.0×10^{-1}
800	38	0-10	9.2×10^{-1}	8.9×10^{-1}	9.8×10^{-1}	5.4×10^{-1}
800	46	0-10	8.1×10^{-1}	8.7×10^{-1}	1.1	4.7×10^{-1}
800	30	30-35	1.3	1.4	1.8	4.1×10^{-1}
800	41	30-35	1.6	1.9	2.5	5.8×10^{-1}
800	46	30-35	2.1	2.1	2.7	5.6×10^{-1}
800	30	50-52	2.0	1.6	1.8	9.9×10^{-1}
800	46	50-52	3.4	2.9	3.5	1.0
2000	46	0-10	1.1	1.0×10^{-1}	1.0	9.4×10^{-1}
2000	46	30-35	2.4	2.6	3.2	1.1
2000	46	50-52	3.4	3.2	3.6	1.8
5000	46	30-35	3.5	3.2	3.1	2.9
5000	46	50-52	3.7	3.6	3.1	3.6

TABLE IX

T_t	E_m^i	J^i	$q_E/\pi b^2_{max}$
800	46	0-10	0.65
800	30	30-35	0.62
800	41	30-35	0.68
800	46	30-35	0.71
800	30	50-52	0.74
800	46	50-52	0.84
2000	46	0-10	0.56
2000	46	30-35	0.67
2000	46	50-52	0.76
5000	46	30-35	0.65
5000	46	50-52	0.84

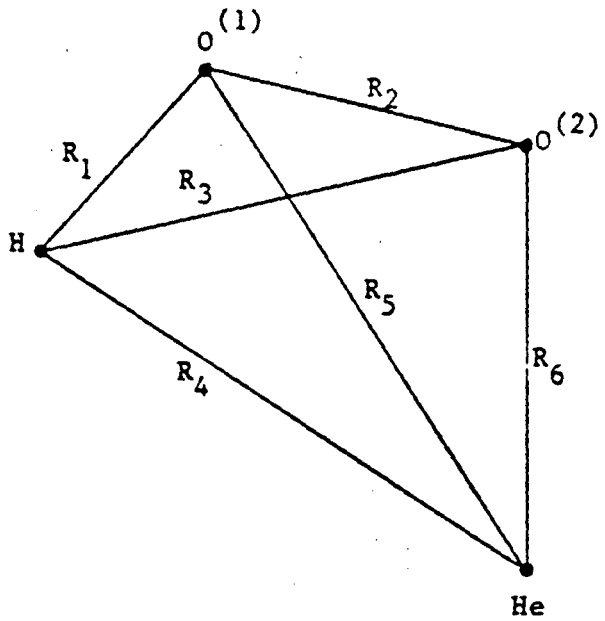

Fig. 1

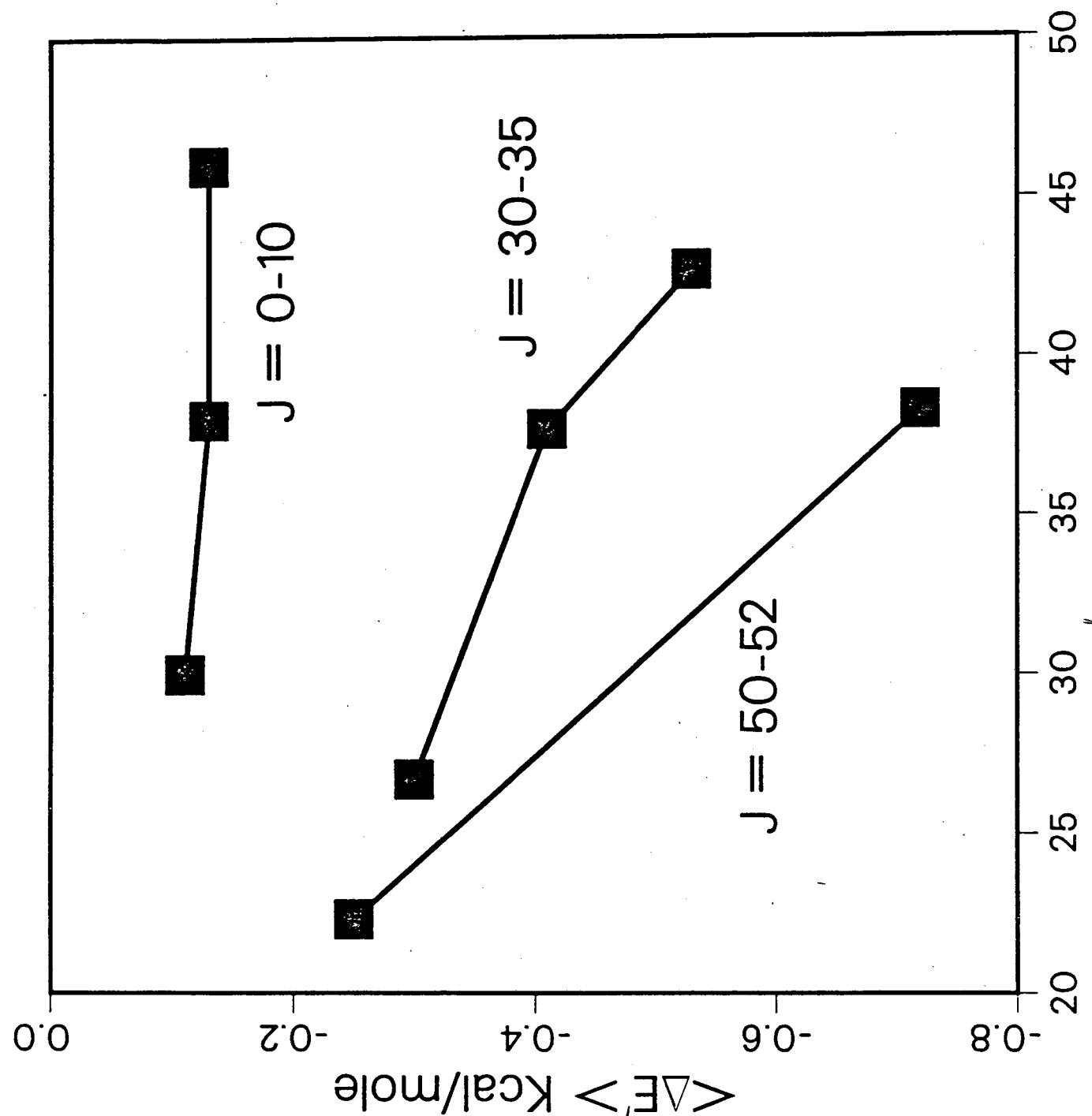
J = 0-10
J = 30-35
J = 50-52
<ΔE'> Kcal/mole
E' (Kcal/mole)
0.0
-0.2
-0.4
-0.6
-0.8
20
25
30
35
40
45
50

Fig. 2

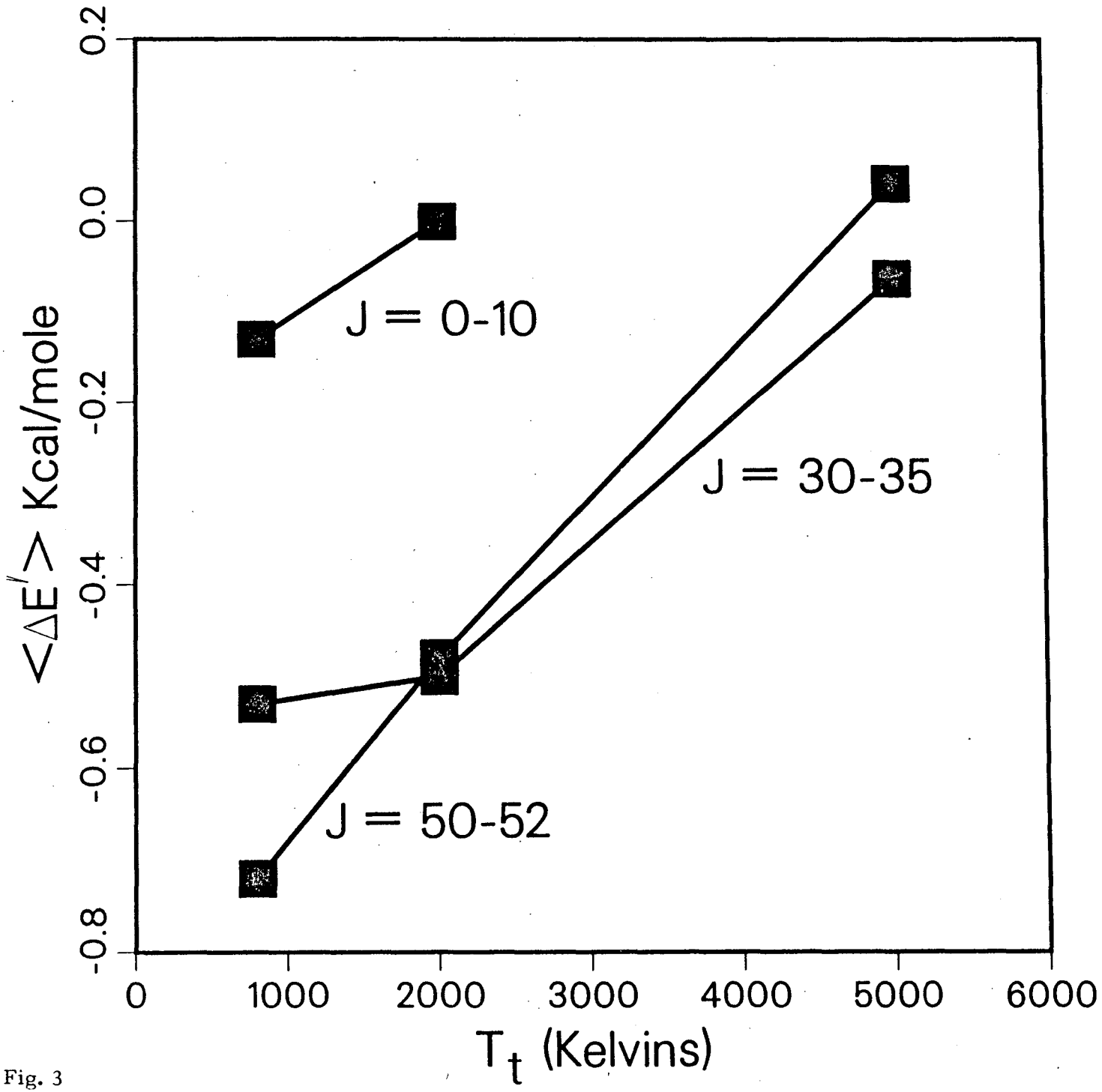
0.2
0.0
-0.2
-0.4
-0.6
-0.8
$\langle \Delta E' \rangle$ Kcal/mole
J = 0-10
J = 30-35
J = 50-52
0
1000
2000
3000
4000
5000
6000
T_t (Kelvins)

Fig. 3

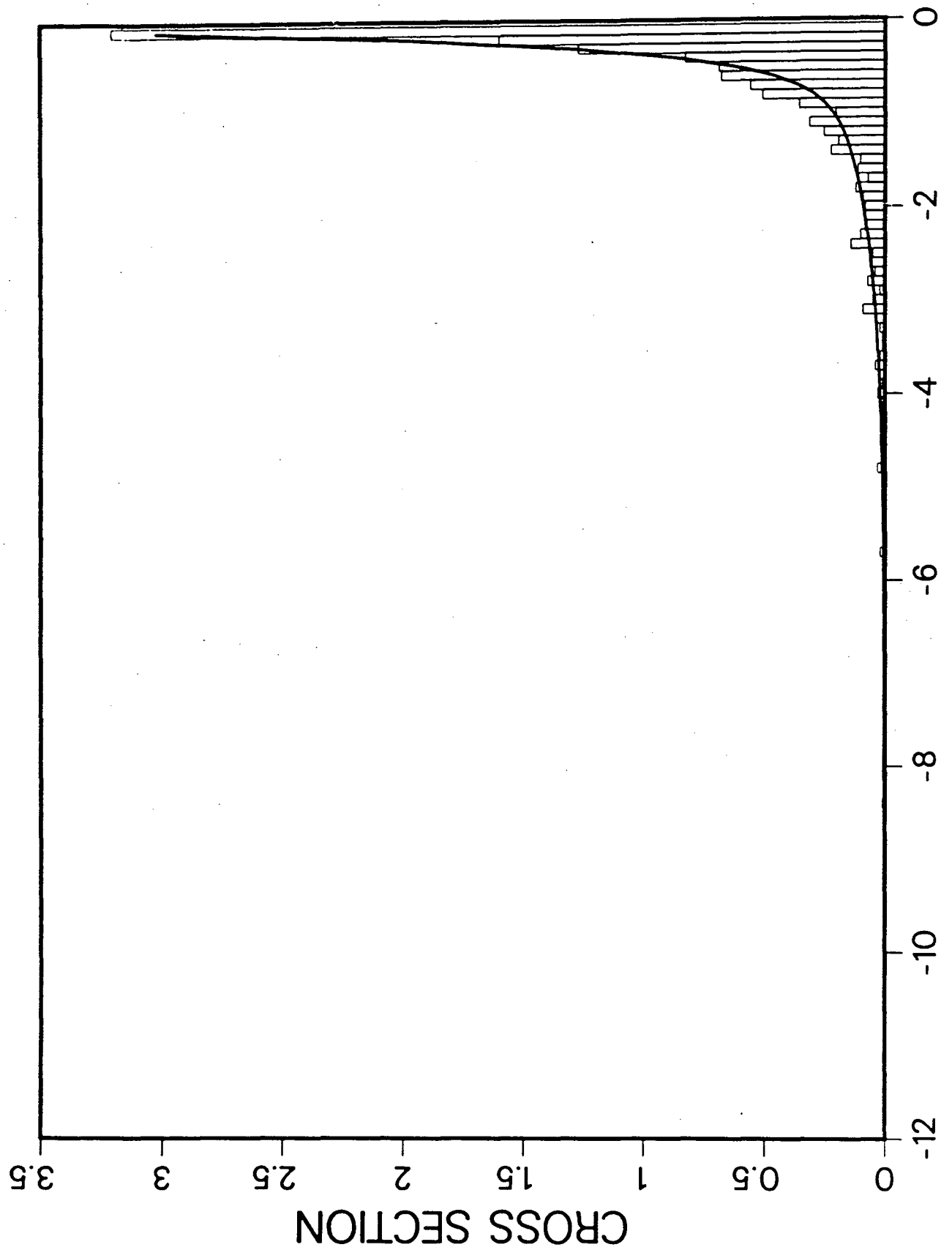

Fig. 4

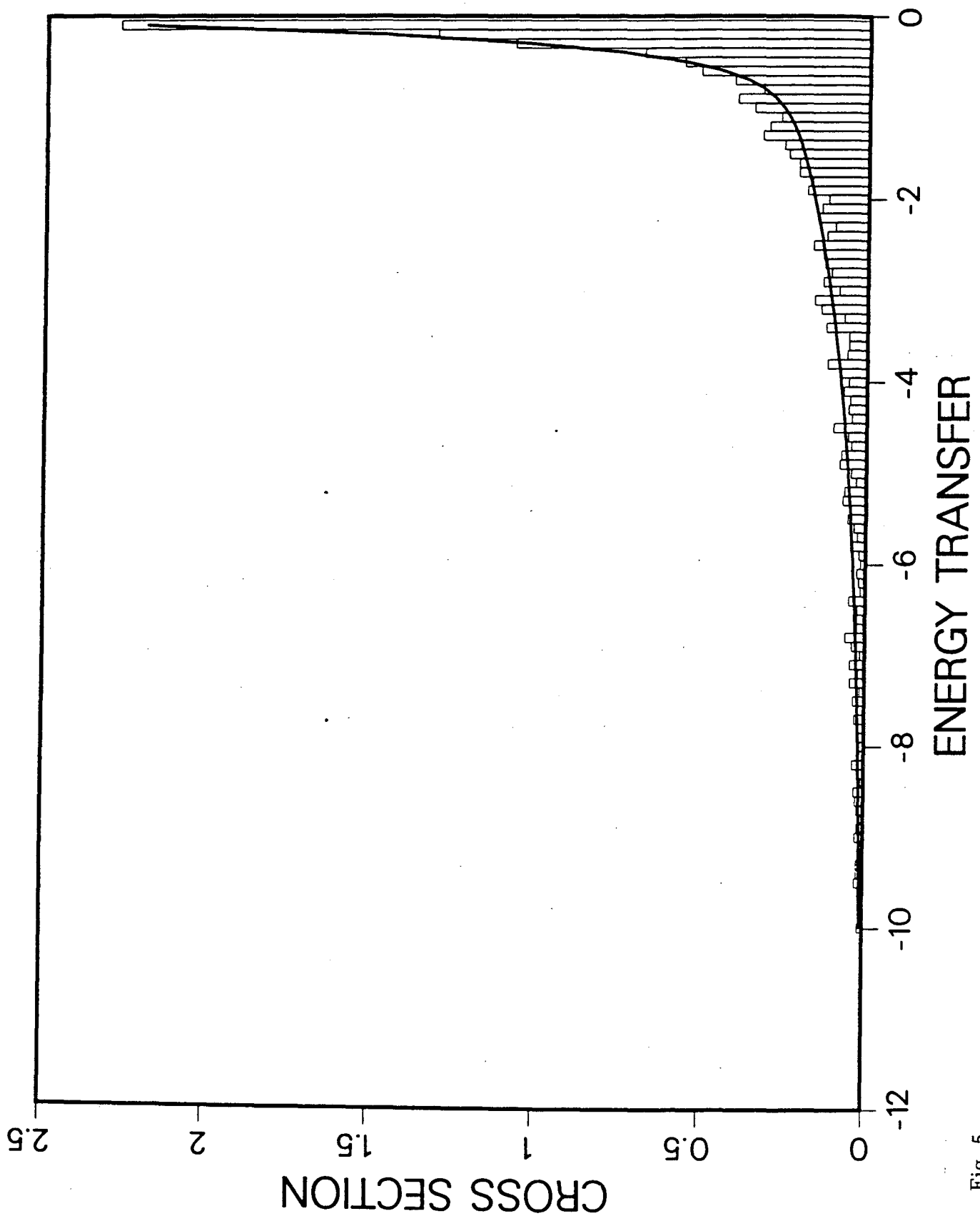

Fig. 5

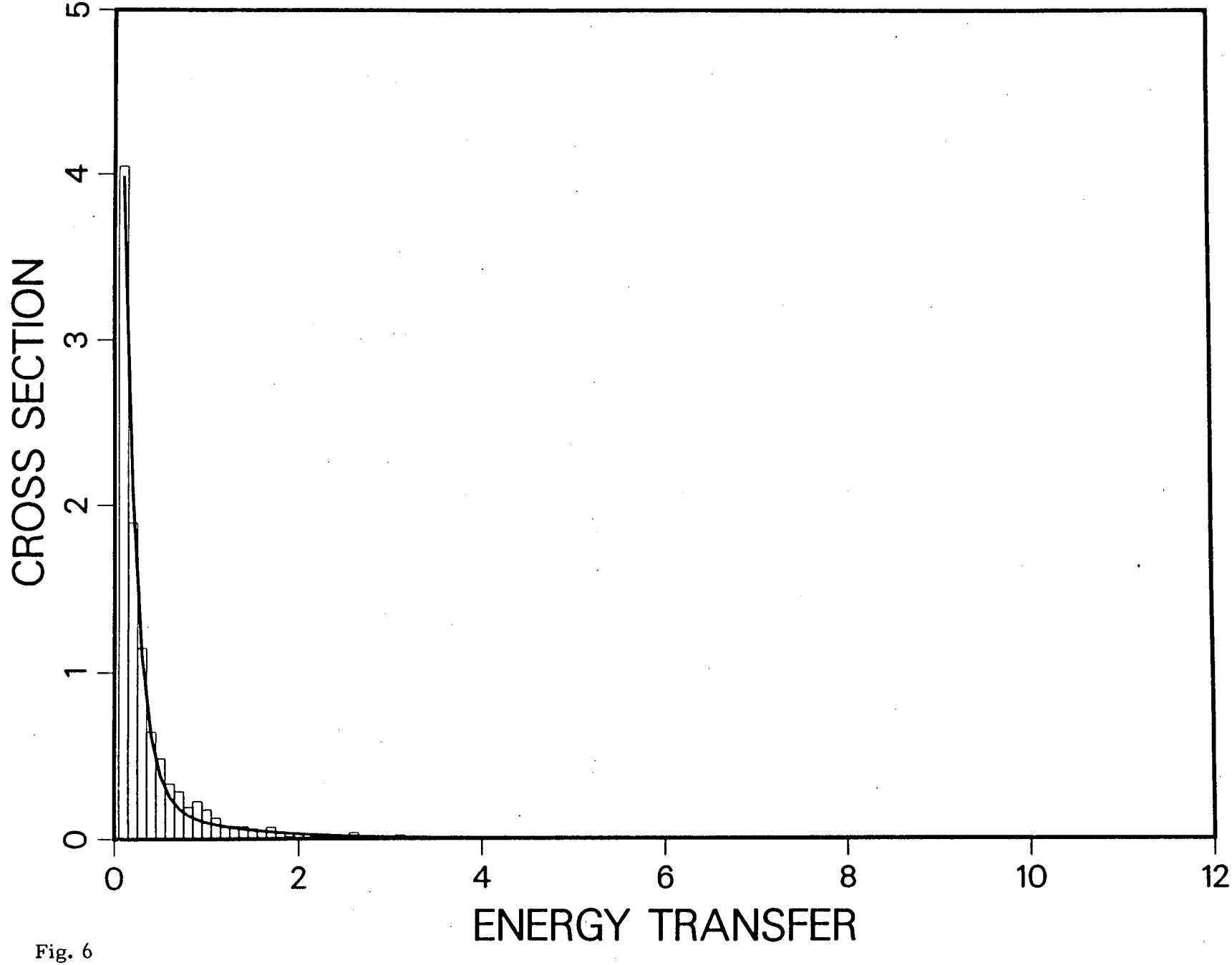

Fig. 6

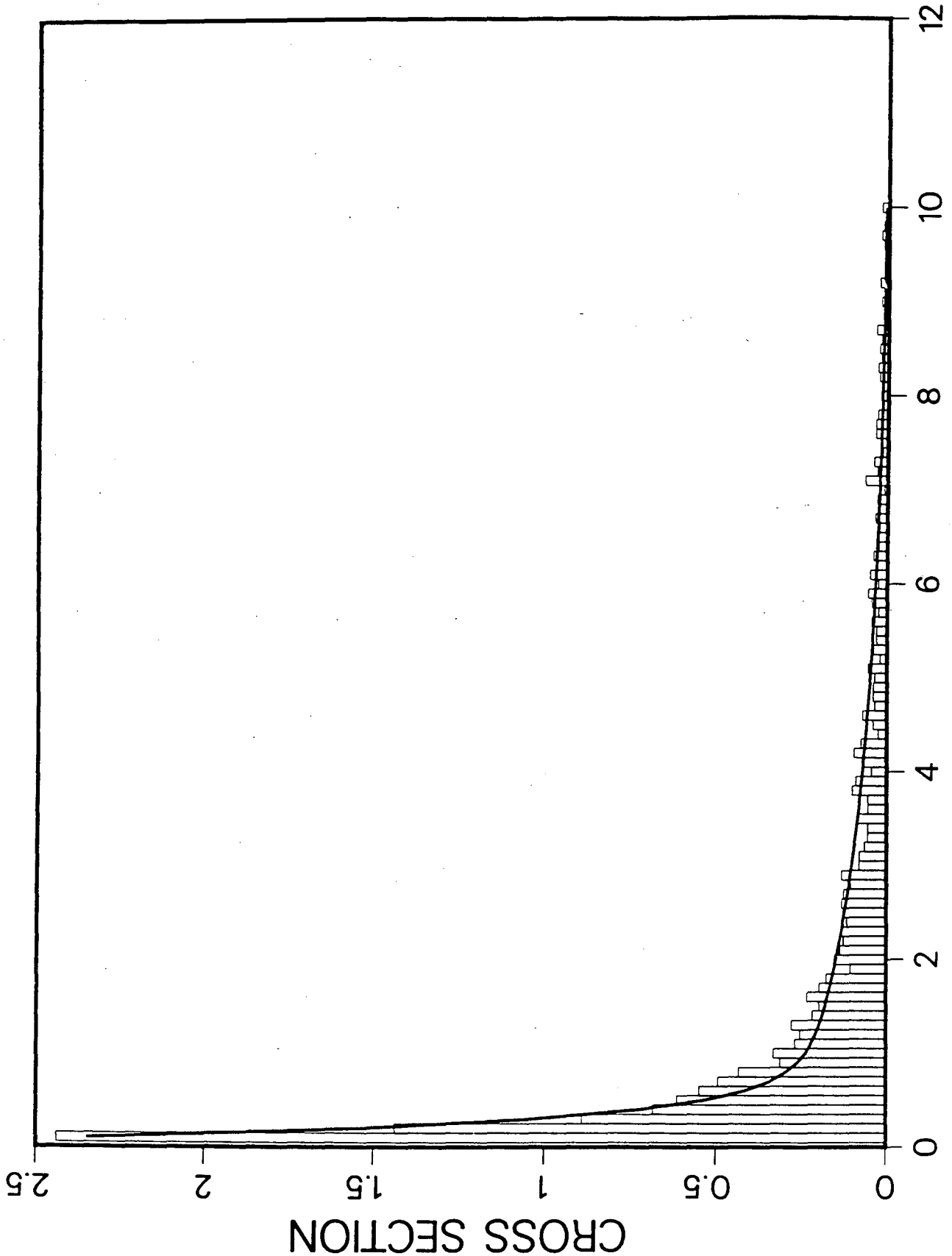

Fig. 7

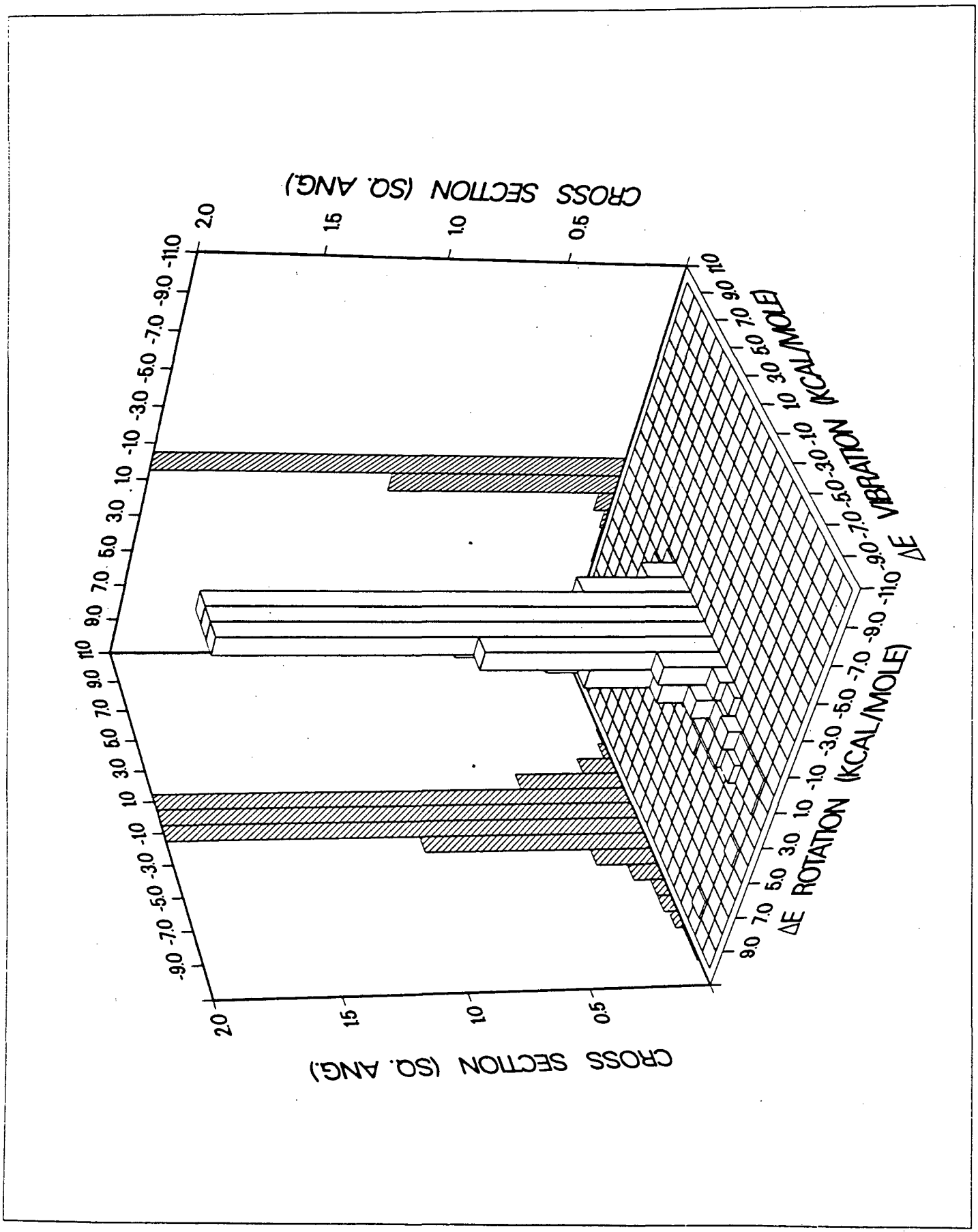
CROSS SECTION (SQ. ANG.)
2.0
1.5
1.0
0.5
ΔE ROTATION (KCAL/MOLE)
ΔE VIBRATION (KCAL/MOLE)

Fig. 8

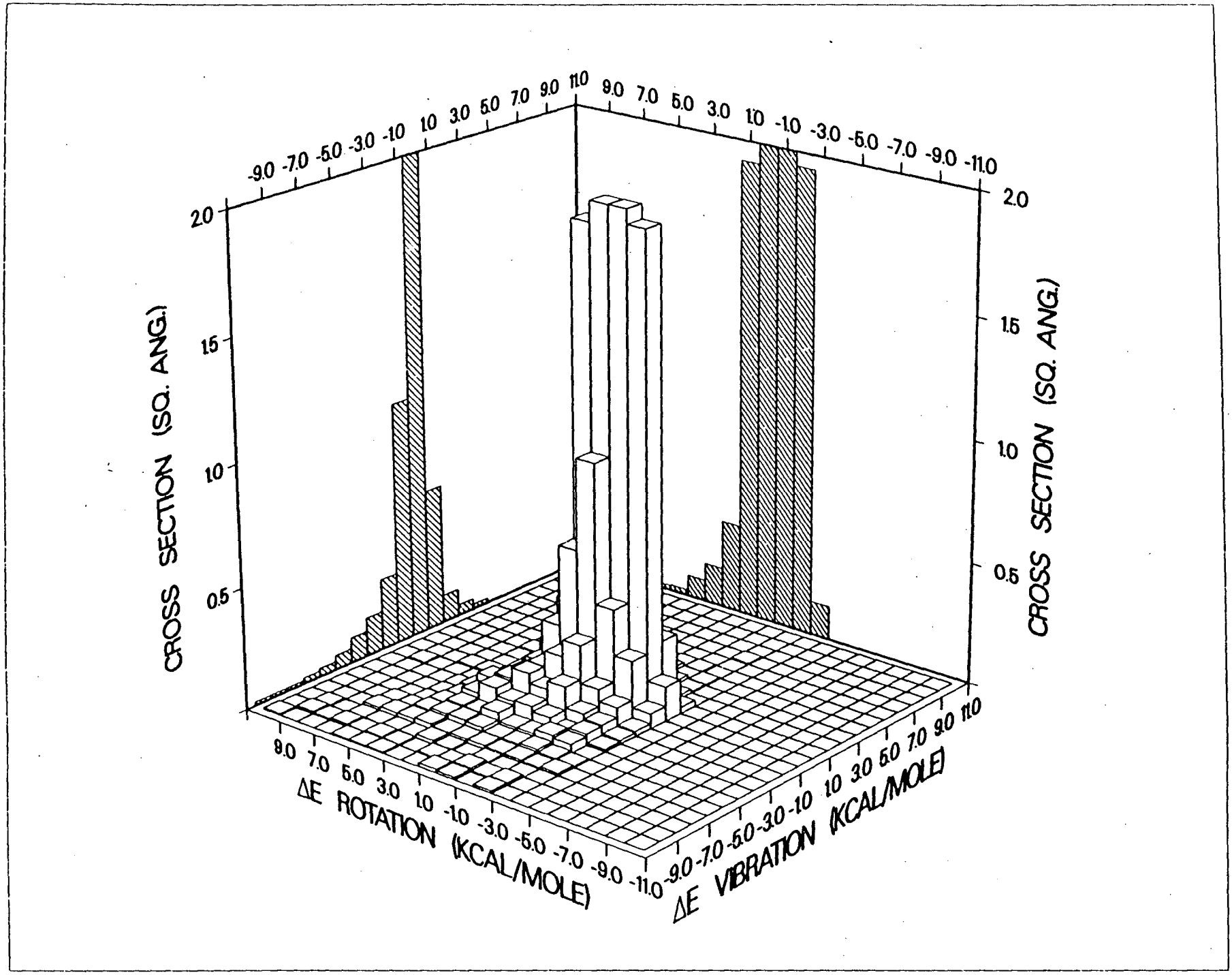
CROSS SECTION (SQ. ANG.)
2.0
1.5
1.0
0.5
-9.0 -7.0 -5.0 -3.0 -1.0 1.0 3.0 5.0 7.0 9.0 11.0
9.0 7.0 5.0 3.0 1.0 -1.0 -3.0 -5.0 -7.0 -9.0 -11.0
ΔE ROTATION (KCAL/MOLE)
ΔE VIBRATION (KCAL/MOLE)
CROSS SECTION (SQ. ANG.)

Fig. 9

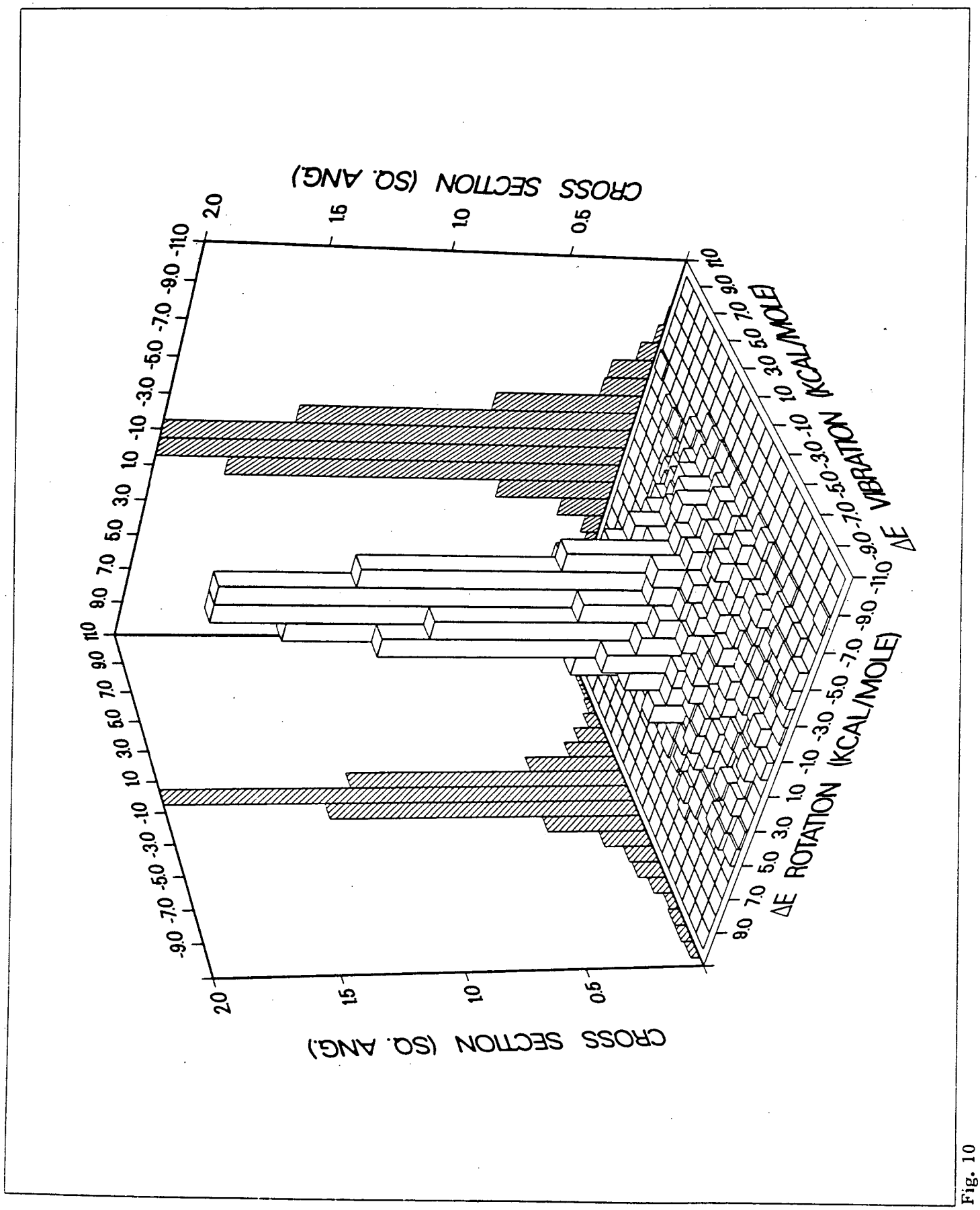
CROSS SECTION (SQ. ANG.)
2.0
1.5
1.0
0.5
ΔE ROTATION (KCAL/MOLE)
ΔE VIBRATION (KCAL/MOLE)
-11.0 -9.0 -7.0 -5.0 -3.0 -1.0 1.0 3.0 5.0 7.0 9.0 11.0

Fig. 10

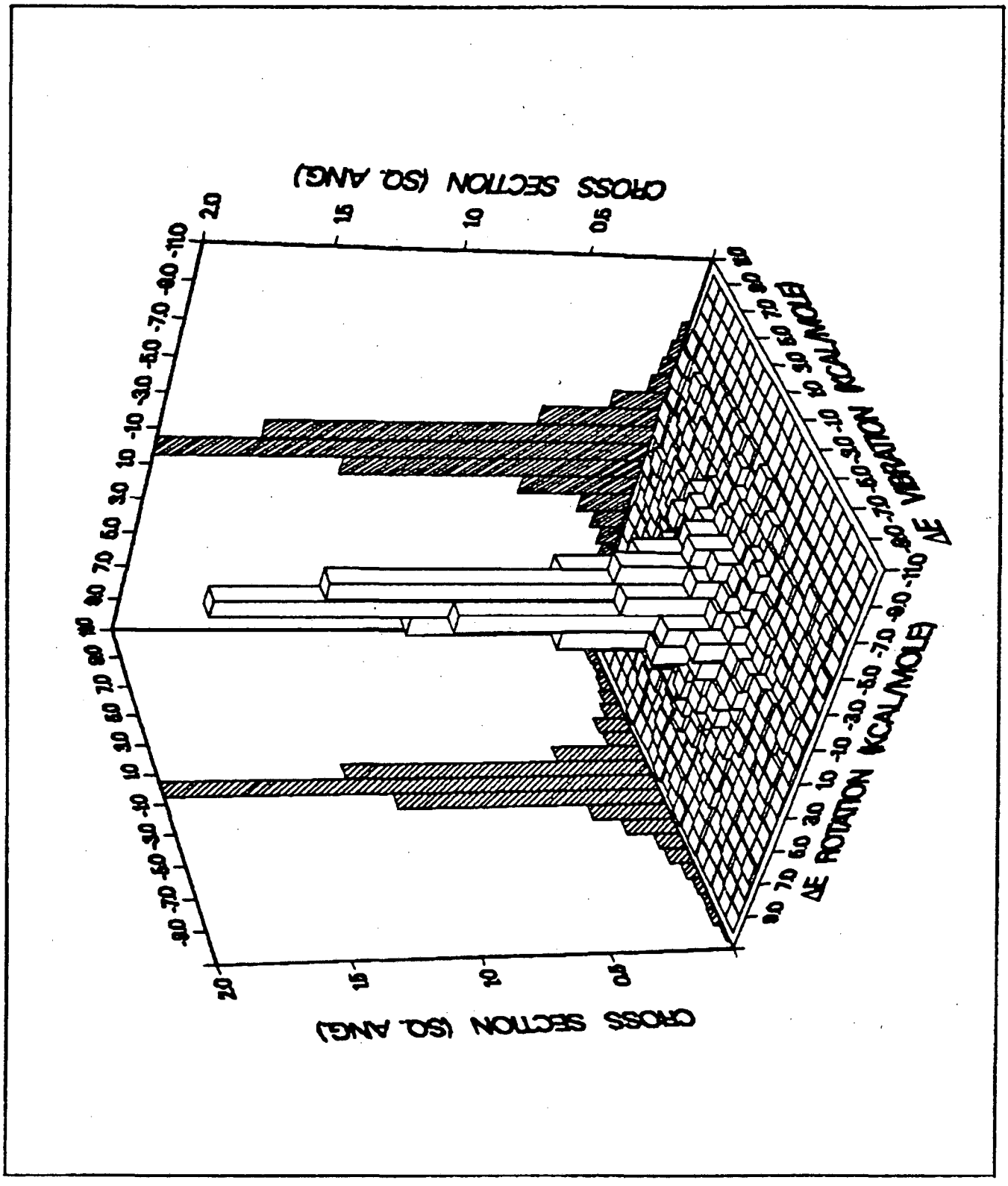
CROSS SECTION (SQ. ANG)
CROSS SECTION (SQ. ANG)
ΔE ROTATION KCAL/MOLE
ΔE VIBRATION KCAL/MOLE

Fig. 11

TECHNICAL INFORMATION DEPARTMENT
LAWRENCE BERKELEY LABORATORY
UNIVERSITY OF CALIFORNIA
BERKELEY, CALIFORNIA 94720